Propagation characteristics of fast light in an erbium-doped fiber amplifier

Senfar Wen[1,2,*] and Sien Chi[3,4]

[1]*Institute of Electrical Engineering, Chung Hua University, 30 Tung Shiang, Hsinchu, Taiwan 300, China*
[2]*Institute of Engineering Science, Chung Hua University, 30 Tung Shiang, Hsinchu, Taiwan 300, China*
[3]*Department of Photonics and Institute of Electro-Optical Engineering, National Chiao Tung University, 1001 Ta Hsueh Road, Hsinchu, Taiwan 300, China*
[4]*Department of Electrical Engineering, Yuan Ze University, 135 Yuandong Road, Chungli, Taiwan 320, China*
**Corresponding author: swen@chu.edu.tw*

Received October 25, 2007; revised April 9, 2008; accepted April 16, 2008;
posted April 18, 2008 (Doc. ID 88998); published May 29, 2008

A perturbation method is used to study the interactions among the signal power, pump power, and metastable population density for fast light in an erbium-doped fiber amplifier. The impact of temporal pump depletion (TPD) on fast light is investigated in which TPD is the response of the pump power to the temporal variation of the metastable population density. It is found that the gain coefficient and the absolute value of the negative group velocity are overestimated without considering the TPD. The effects of high-order dispersions on fast light are also shown. © 2008 Optical Society of America

OCIS codes: 260.2030, 060.2320.

1. INTRODUCTION

The propagation of an optical pulse in the highly dispersive medium for slow or fast light was intensively investigated [1–10]. It was reported that slow and fast light can be observed by using the effect of coherent population oscillation (CPO) in an erbium-doped fiber amplifier (EDFA) [9,10]. Due to the interaction between the fields and the erbium ions in an EDFA, there is the spectral gain dip of a narrow bandwidth. According to the Kramers–Kronig relations, the EDFA becomes a highly dispersive medium for the pulse in the presence of a gain dip. The spectral gain dip provides the dispersion for fast light. The case of a 9 m erbium-doped fiber strongly pumped by a 980 nm semiconductor laser diode was shown in [10]. The 1550 nm input pulse of 0.5 ms in width and 0.5 mW in power superimposed on a strong continuous wave (cw) control beam of the same wavelength was launched into the EDFA. The pulse backward propagation owing to a negative group velocity was reported to be experimentally observed. The group index of the pulse is estimated to be about −4000.

Because the interested pulse width is much longer than the polarization dephasing time, the interaction of the pulse and the population of the doped erbium ions in an EDFA can be described by the coupled equations of power evolution equation and rate equation. A perturbation method to derive the time delay and gain (loss) coefficient of a sinusoidally modulated wave was used in [9]. This method linearizes the coupled equations by assuming that the power of the sinusoidally modulated wave is much less than that of the control beam. Under this assumption, the temporal variation of the population inversion induced by the sinusoidally modulated wave can also be assumed to be much less than the steady-state population inversion induced by the control beam. From the linearized coupled equations, the gain coefficient and group velocity of the sinusoidally modulated wave can be derived. However, in this paper, we show that this perturbation method is not accurate in an EDFA even for the case that the assumption of perturbation is valid. The numerical results solved from the complete coupled equations without linearization show that the gain coefficient and the absolute value of the negative group velocity are overestimated.

We find that the inaccuracy is due to the temporal pump depletion (TPD) that is not included in the above perturbation method. The pump power depleted by the control beam is not time varying. An optical pulse depletes the metastable population density. The pump power is absorbed more when the metastable population density is depleted. The TPD is the pump power temporal variation responding to the temporal variation of the metastable population density absorbed by the optical pulse. In this paper, we develop the perturbation method including the TPD effect. It is shown that our method is accurate compared with the results directly solved from the complete coupled equations. The impact of the TPD on the gain coefficient and group velocity is shown. In addition, the pulse delay time and pulse shape distortion resulting from high-order dispersions induced by CPO in an EDFA are also studied.

2. COUPLED EQUATIONS

The energy levels of an EDFA can be approximated as a three-level system. However the decay rate from the upper level to the metastable level is much faster than the decay rate from the metastable level to the ground level. Because the population density of the upper level is neg-

ligible, the signal and pump powers in an EDFA can be described by the following equations [11]:

$$\frac{\partial P_s}{\partial z} + \frac{n_{gs}}{c}\frac{\partial P_s}{\partial t} = -(\alpha_s + \alpha_{ls})P_s + (\alpha_{gs} + \alpha_{ls})N_2 P_s, \quad (1)$$

$$\frac{\partial P_p}{\partial z} + \frac{n_{gp}}{c}\frac{\partial P_p}{\partial t} = -(\alpha_p + \alpha_{lp})P_p + (\alpha_{gp} + \alpha_{lp})N_2 P_p, \quad (2)$$

where P_s is the signal power including the pulse and control beam powers; P_p is the forward pump power; n_{gs} and n_{gp} are the group indexes of the signal and pump in the absence of doped erbium ions, respectively; c is the light velocity in vacuum; α_s and α_p are the intrinsic fiber loss coefficients at the signal and pump wavelengths, respectively; α_{ls} and α_{lp} are the absorption coefficients at the signal and pump wavelengths, respectively, which are due to doped erbium ions when population is completely in the ground level; α_{gs} and α_{gp} are the gain coefficients at the signal and pump wavelengths, respectively, which are due to doped erbium ions when population is completely in the metastable level. In Eqs. (1) and (2), $N_2 = n_2/n_t$ is the normalized metastable population density in which n_2 and n_t are the population density of the metastable level and the doping density, respectively.

The normalized metastable population density can be described by the rate equation [11],

$$\frac{dN_2}{dt} = \frac{1}{\tau}\left(\frac{P_s}{P_s^{th}} + \frac{P_p}{P_p^{th}}\right) - \frac{1}{\tau}\left(1 + \frac{P_s}{P_s^{is}} + \frac{P_p}{P_p^{is}}\right)N_2, \quad (3)$$

where τ is the lifetime of the metastable level and

$$P_k^{th} = \frac{A_e h\nu_k n_t}{\alpha_{lk}\tau}, \quad (4a)$$

$$P_k^{is} = \frac{A_e h\nu_k n_t}{(\alpha_{gk} + \alpha_{lk})\tau}, \quad (4b)$$

where $k = s$ and p; $h\nu_s$ and $h\nu_p$ are the photon energies of the signal and pump, respectively; and A_e is the effective doping area.

Equations (1)–(3) are the coupled equations that describe the interaction of the optical fields and doped erbium ions. The coupled equations can be numerically solved with the initial conditions

$$P_s(z = 0, t) = P_{c0} + P_{a0}(t), \quad (5)$$

$$P_p(z = 0, t) = P_{p0}, \quad (6)$$

where P_{c0} is the input control beam power, $P_{a0}(t)$ is the input pulse power envelope; and P_{p0} is the input forward pump power. In this paper, we will consider the Gaussian input pulse

$$P_{a0}(t) = P_{s0}\exp[-(t/T_0)^2], \quad (7)$$

where P_{s0} is the pulse peak power and the FWHM pulse width $T_w = 2[\ln(2)]^{1/2}T_0$.

For the considered EDFA, $\tau = 10.5$ ms, $A_e = 3.14\ \mu m^2$, $n_t = 1\times10^{25}\ m^{-3}$, the absorption cross section at 980 nm in wavelength is 2.1×10^{-25} m, the absorption and emission cross sections at 1550 nm in wavelength are 3.2×10^{-25} m and 3.78×10^{-25} m, respectively, and the EDFA length $L = 10$ m. At 980 nm in wavelength, $\alpha_p = 1.7$ dB/km, $\alpha_{lp} = 4.52$ dB/m, and $\alpha_{gp} = 0$. At 1550 nm in wavelength, $\alpha_s = 0.4$ dB/km, $\alpha_{ls} = 3.11$ dB/m, and $\alpha_{gs} = 3.67$ dB/m. Since the delay time contributed from the group index $n_g = 1.5$ in an EDFA is $Ln_g/c = 50$ ns, which is much less than the interested millisecond pulse width, the terms with n_{gs} and n_{gp} in Eqs. (1) and (2), respectively, are negligible. We take the pulse width $T_w = 0.5$ ms and the pump power $P_{p0} = 180$ mW to show the numerical results in Section 4, where the control beam power P_{c0} and the peak power P_{s0} are varied.

3. PERTURBATIVE SOLUTION

The signal power along the EDFA can be written as $P_s(z,t) = P_c(z) + P_a(z,t)$. For the CPO effect, the pulse power $P_a(z,t)$ is much less than the control beam power $P_c(z)$ [12], i.e., $P_c(z) \gg |P_a(z,t)|$. For simplicity the z dependence of all variables will not be shown in the following, unless they are specified. The normalized metastable population density can be written as $N_2(t) = N_c + N_a(t)$, where N_c and $N_a(t)$ are the normalized metastable population densities corresponding to P_c and $P_a(t)$, respectively, hence $|N_c| \gg |N_a(t)|$. The signal power depletes the pump power through the metastable population density. The corresponding pump power can be written as $P_p(t) = P_{pc} + P_{pa}(t)$, where P_{pc} and $P_{pa}(t)$ are the pump powers corresponding to N_c and $N_a(t)$, respectively, hence $P_{pc} \gg |P_{pa}(t)|$. The powers and normalized metastable population density can be written as

$$P_s(t) = P_c + \int \tilde{P}_a(\Omega)\exp(-i\Omega t)d\Omega, \quad (8)$$

$$P_p(t) = P_{pc} + \int \tilde{P}_{pa}(\Omega)\exp(-i\Omega t)d\Omega, \quad (9)$$

$$N_2(t) = N_c + \int \tilde{N}_a(\Omega)\exp(-i\Omega t)d\Omega, \quad (10)$$

where $\tilde{P}_a(\Omega)$, $\tilde{P}_{pa}(\Omega)$, and $\tilde{N}_a(\Omega)$ are the Fourier transforms of $P_a(t)$, $P_{pa}(t)$, and $N_a(t)$, respectively. Note that $\tilde{P}_a(\Omega)$ and $\tilde{P}_{pa}(\Omega)$ are the spectra of the power envelopes. Because $P_a(t)$, $P_{pa}(t)$, and $N_a(t)$ are real, we have the relations $\tilde{P}_a(\Omega) = \tilde{P}_a*(-\Omega)$, $\tilde{P}_{pa}(\Omega) = \tilde{P}_{pa}*(-\Omega)$, and $\tilde{N}_a(\Omega) = \tilde{N}_a*(-\Omega)$.

Substituting Eqs. (8)–(10) into Eq. (3) and equating the terms of the same order of magnitude, we have

$$N_c = \left(\frac{P_c}{P_s^{th}} + \frac{P_{pc}}{P_p^{th}}\right)(\omega_c\tau)^{-1}, \quad (11)$$

$$\tilde{N}_a(\Omega) = \left[\left(\frac{\tilde{P}_a}{P_s^{th}} + \frac{\tilde{P}_{pa}}{P_p^{th}}\right) - \left(\frac{\tilde{P}_a}{P_s^{is}} + \frac{\tilde{P}_{pa}}{P_p^{is}}\right)N_c\right](\omega_c\tau - i\Omega\tau)^{-1}, \quad (12)$$

where ω_c is the resonant angular frequency defined according to [9] and

$$\omega_c = \left(1 + \frac{P_c}{P_s^{is}} + \frac{P_{pc}}{P_p^{is}}\right)\tau^{-1}. \quad (13)$$

Substituting Eqs. (8)–(12) into Eqs. (1) and (2) and equating the terms of the same order of magnitude, we have the coupled equations

$$\frac{dP_c}{dz} = -(\alpha_s + \alpha_{ls})P_c + (\alpha_{gs} + \alpha_{ls})N_c P_c, \quad (14)$$

$$\frac{dP_{pc}}{dz} = -(\alpha_p + \alpha_{lp})P_{pc} + (\alpha_{gp} + \alpha_{lp})N_c P_{pc}, \quad (15)$$

$$\frac{d\tilde{P}_a(\Omega)}{dz} = c_{ss}\tilde{P}_a(\Omega) + c_{sp}\tilde{P}_{pa}(\Omega), \quad (16)$$

$$\frac{d\tilde{P}_{pa}(\Omega)}{dz} = c_{pp}\tilde{P}_{pa}(\Omega) + c_{ps}\tilde{P}_a(\Omega), \quad (17)$$

where the coefficients

$$c_{ss} = i\frac{n_{gs}}{c}\Omega - (\alpha_s + \alpha_{ls}) + (\alpha_{gs} + \alpha_{ls})\left[N_c + \left(\frac{P_c}{P_s^{th}} - \frac{P_c}{P_s^{is}}N_c\right)(\omega_c\tau - i\Omega\tau)^{-1}\right], \quad (18)$$

$$c_{sp} = (\alpha_{gs} + \alpha_{ls})\left(\frac{P_c}{P_p^{th}} - \frac{P_c}{P_p^{is}}N_c\right)(\omega_c\tau - i\Omega\tau)^{-1}, \quad (19)$$

$$c_{pp} = i\frac{n_{gp}}{c}\Omega - (\alpha_p + \alpha_{lp}) + (\alpha_{gp} + \alpha_{lp})\left[N_c + \left(\frac{P_{pc}}{P_p^{th}} - \frac{P_{pc}}{P_p^{is}}N_c\right)\times(\omega_c\tau - i\Omega\tau)^{-1}\right], \quad (20)$$

$$c_{ps} = (\alpha_{gp} + \alpha_{lp})\left(\frac{P_{pc}}{P_s^{th}} - \frac{P_{pc}}{P_s^{is}}N_c\right)(\omega_c\tau - i\Omega\tau)^{-1}. \quad (21)$$

For the case without TPD, the gain coefficient and propagation constant of $\tilde{P}_a(\Omega)$ are the real and imaginary parts of c_{ss}, respectively. "Propagation constant" usually refers to the electric field, but for the present analysis it refers to the power envelope. The group index of $P_a(t)$ can be obtained from the derivative of the propagation constant with respect to Ω at $\Omega=0$. However, TPD always exists. Thus, the gain coefficient and propagation constant of $\tilde{P}_a(\Omega)$ must be solved from the coupled Eqs. (14)–(17). The following shows the numerical solving procedures.

Step 1. The cw powers P_c and P_{pc} along the EDFA are solved from Eqs. (14) and (15) with the boundary conditions $P_c(z=0)=P_{c0}$ and $P_{pc}(z=0)=P_{p0}$ in which N_c is given by Eq. (11). Note that Eqs. (14) and (15) are independent of Eqs. (16) and (17).

Step 2. $\tilde{P}_a(z,\Omega)$ and $\tilde{P}_{pa}(z,\Omega)$ are solved from Eqs. (16) and (17) with the boundary conditions $\tilde{P}_a(z=0,\Omega)=\tilde{P}_{a0}(\Omega)$ and $\tilde{P}_{pa}(z=0,\Omega)=0$, where $\tilde{P}_{a0}(\Omega)$ is the Fourier transform of the input pulse envelope $P_{a0}(t)$, and there is no initial temporal pump power variation. Note that the coefficients given by Eqs. (18)–(21) along the EDFA require the cw powers P_c and P_{pc} solved in Step 1. The approximate solutions of the pulse shape and temporal pump power variation are

$$P_a(z,t) = \int \tilde{P}_a(z,\Omega)\exp(-i\Omega t)d\Omega, \quad (22)$$

$$P_{pa}(z,t) = \int \tilde{P}_{pa}(z,\Omega)\exp(-i\Omega t)d\Omega, \quad (23)$$

respectively. The integration of Eqs. (22) and (23) can be numerically calculated with an inverse fast Fourier transform (FFT) routine.

Step 3. Because the coupled Eqs. (16) and (17) are linear, we define the spectral transmittance of the pulse envelope at the distance z as $T(z,\Omega)=\tilde{P}_a(z,\Omega)/\tilde{P}_{a0}(\Omega)$, which can be written as $T(z,\Omega)=|T(z,\Omega)|\exp[i\theta(z,\Omega)]$, and $\theta(z,\Omega)$ is the phase of $T(z,\Omega)$. The gain coefficient and propagation constant of the spectral component of the pulse envelope are $g_a(z,\Omega)=d\ln(|T(z,\Omega)|)/dz$ and $\beta_a(z,\Omega)=d\theta(z,\Omega)/dz$, respectively.

The group delay time along the EDFA evaluated at $\Omega=0$ is $T_{d0}(z)=d\theta(z,\Omega)/dz|_{\Omega=0}$. However, the actual pulse delay time should be evaluated from the pulse shape given by Eq. (22). We will show in Section 4 that the actual pulse delay time is significantly influenced by high-order dispersions.

At the output of the EDFA, the accumulated gain $\gamma_a(\Omega)=\ln(|T(z=L,\Omega)|)$ and the phase shift $\phi_a(\Omega)=\theta(z=L,\Omega)$. The gain coefficient and propagation constant are even and odd functions, respectively, for the CPO in a two-level system [12]. In Section 4, it is shown that $\gamma_a(\Omega)$ and $\phi_a(\Omega)$ are also even and odd functions, respectively. Thus we may expand them as

$$\gamma_a(\Omega) + i\phi_a(\Omega) = \sum_{\substack{k=0 \\ k:\text{even}}}^{Q}\frac{1}{k!}\gamma_{ak}\Omega^k + i\sum_{\substack{k=1 \\ k:\text{odd}}}^{Q}\frac{1}{k!}\phi_{ak}\Omega^k, \quad (24)$$

where Q is an integer; γ_{ak} and ϕ_{ak} are the coefficients obtained by numerically fitting $\gamma_a(\Omega)$and $\phi_a(\Omega)$ with Eq. (24). For the cases considered in this paper, we take $Q=29$ so that $\gamma_a(\Omega)$ and $\phi_a(\Omega)$ can be fitted well. γ_{ak} and ϕ_{ak} represent dispersion coefficients that are the derivatives of $\gamma_a(\Omega)$ and $\phi_a(\Omega)$ at $\Omega=0$, respectively. It is noticed that $\phi_{a1}=T_{d0}(z=L)$. In Eq. (24), the even and odd order terms can be called the gain dispersion and phase shift dispersion, respectively. For studying the effect of dispersion induced by CPO on the pulse shape, we define the output pulse shape:

$$P_a^{(M)}(t) = \int \tilde{P}_{a0}(\Omega)\exp[\gamma_a^{(M)}(\Omega) + i\phi_a^{(M)}(\Omega) - i\Omega t]\mathrm{d}\Omega, \tag{25}$$

where M is an integer not larger than Q; $\gamma_a^{(M)}(\Omega)$ and $\phi_a^{(M)}(\Omega)$ are the partial accumulated gain and phase shift including the dispersions up to the Mth order, respectively, i.e., they are the accumulated gain and phase shift given in Eq. (24) except that the terms of order larger than M are dropped. Comparing the pulse shapes of $P_a^{(M)}\times(t)$ and $P_a^{(M-1)}(t)$, one can clearly see the effect of the Mth order dispersion on the pulse shape.

For the case without TPD, we may solve Eqs. (14) and (16) with the coefficient $c_{sp}=0$. From the solutions, the output pulse shape, gain coefficient, and propagation constant can be calculated with similar methods as shown above.

4. NUMERICAL RESULTS

It is found that the approximate solutions solved from Eqs. (14)–(17) are nearly the same as the exact solutions solved from Eqs. (1)–(3) when the control beam power P_{c0} is about 100 times larger than the peak pulse power P_{s0}. In this section, we take the ratio $P_{c0}/P_{s0}=10$ [10], which

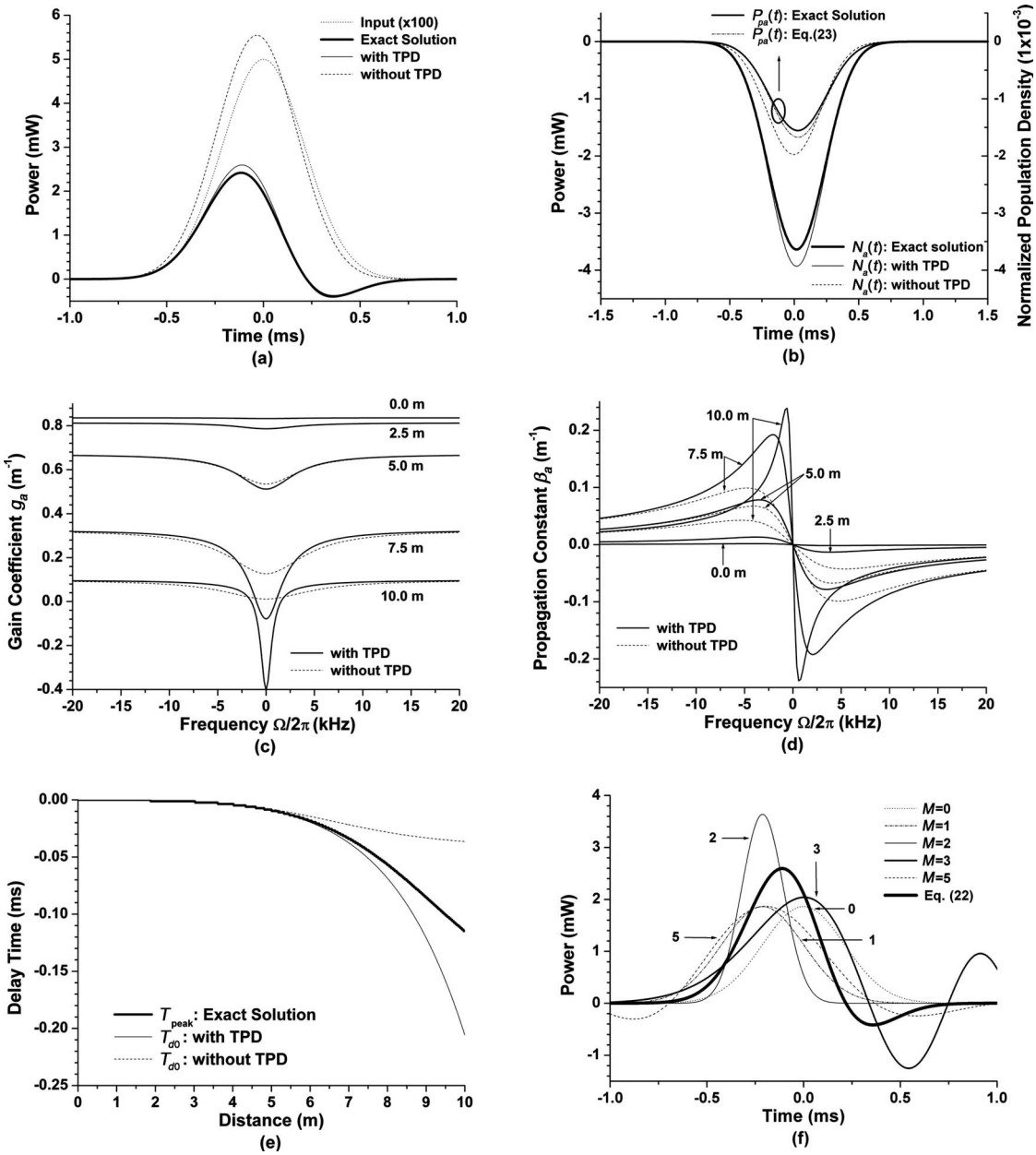

Fig. 1. With input control beam power $P_{c0}=0.5$ mW, (a) input and output pulse shapes, (b) pump power temporal variation and normalized metastable population density at EDFA output end, (c) gain coefficient spectra at several distances, (d) propagation constant spectra at several distances, (e) peak-power delay time T_{peak} and the group delay time T_{d0} along the EDFA evaluated at $\Omega=0$, and (f) output pulse shapes $P_a^{(M)}(t)$ synthesized up to several M dispersion orders and the approximate solution with TPD calculated from Eq. (22) without dispersion expansion. (f) Corresponding values of M (arrows). The exact solution is solved from Eqs. (1)–(3). (a)–(e) Approximate solutions with and without TPD are shown for comparison.

will result in a slight discrepancy between the approximate solution and the exact solution. The propagation characteristics of fast light with $P_{c0}/P_{s0}=10$ and 100 are similar. The cases with $P_{c0}=0.5$, 0.1, and 2.5 mW are considered in Subsections 4.A–4.C.

A. $P_{c0}=0.5$ mW

Figures 1(a)–1(f) show the numerical results with $P_{c0}=0.5$ mW. Figure 1(a) shows the input and output pulse shapes in which the input pulse shape is enlarged 100 times so that it can be clearly shown. The approximate solutions with and without TPD are also shown in Fig. 1(a). Figure 1(a) shows that there is negative power at the tail of the output pulse. The pulse peak power is amplified from 0.05 to 2.42 mW, and the cw power is amplified from 0.5 to 151 mW. Thus the signal power P_s, which comprises both the pulse power P_a and the cw power P_c, at the pulse tail is still amplified. The leading edge of the output pulse depletes the metastable population density. The gain provided by the metastable population density at the pulse tail is lower than that at the pulse leading edge for the signal power. Because the amplified signal power at the pulse tail is less than that at the pulse leading edge, there is the negative power at the pulse tail when the cw power is subtracted from the signal power to derive the pulse shape. This result agrees with the output pulse shape measured in [10]. In Fig. 1(a), one can see that, without TPD, the pulse gain is overestimated, and the absolute value of the pulse delay time is underestimated. The discrepancy between the exact solution and the approximate solution with TPD is due to the pulse peak power that is not small enough compared with the control beam power. Figure 1(b) shows the pump power temporal variation and normalized metastable population density at the EDFA output end in which the approximate solutions $P_{pa}(t)$ and $N_a(t)$ are also shown. $P_{pa}(t)$ and $N_a(t)$are calculated from Eqs. (23) and (12), respectively. For the case without TPD, $\tilde{P}_{pa}=0$ in Eq. (12). One can clearly see that the depletion of the metastable population density is underestimated for the case without considering TPD, which leads to the underestimation of the CPO effect. Figures 1(c) and 1(d) show the gain coefficient and propagation constant spectra, respectively, at several distances. In Figs. 1(c) and 1(d), the approximate solutions with and without TPD are shown. At a 2.5 m distance, the gain coefficient spectra and the propagation constant spectra for the cases with and without TPD are about the same because TPD is not yet significantly built up. After about a 5 m distance, for the case without TPD, the gain coefficient and the absolute value of the negative slope of the propagation constant at $\Omega=0$ are overestimated and underestimated, respectively. Thus the pulse gain and the absolute value of the negative group velocity are overestimated. Figures 2(a) and 2(b) show the accumulated gain and phase shift, respectively, for the approximate solutions with and without TPD. From the results, we study the effect of gain dispersion and phase shift dispersion on pulse propagation in the following.

For the case with TPD shown in Fig. 2(a), the gain dip of narrow bandwidth will result in serious high-order dispersions. The first-order dispersion accelerates fast light without pulse distortion. Higher-order dispersion not only distorts the pulse shape as shown in Fig. 1(a) but also delays the pulse and slows down fast light. Figure 1(e) shows the peak-power delay time T_{peak}, the group delay time T_{d0} with TPD, and the group delay time T_{d0} without TPD. One can see that $|T_{d0}|$ of the case with TPD is much larger than that of the case without TPD. In Fig. 1(e), T_{peak} is only about one-half of T_{d0} with TPD. The average group index can be calculated as $n_{\text{avg}}=cT_d/L$ in which T_d is the delay time. We have $n_{\text{avg}}=-3443$, -6176, and -1093 for $T_d=T_{\text{peak}}$, T_{d0} with TPD, and T_{d0} without TPD, respectively. Figure 1(f) shows the output pulse shapes $P_a^{(M)}(t)$ with partial high-order dispersions, and the cases with $M=0$, 1, 2, 3, and 5 are shown. In Fig. 1(f), the approximate solution with TPD calculated from Eq. (22) without dispersion expansion is also shown for comparison. In Fig. 1(f), one can see how the combined effect of high odd order dispersions slows down fast light. The peak-power delay time of $P_a^{(1)}(t)$ is T_{d0}. The third-order dispersion increases the pulse delay time and slows down fast light. Thus the absolute value of the peak-power delay time is decreased. The fifth-order dispersion accelerates fast light, but it is not able to recover the slow down resulting from the third-order dispersion. The dispersions of order larger than the fifth order further slightly in-

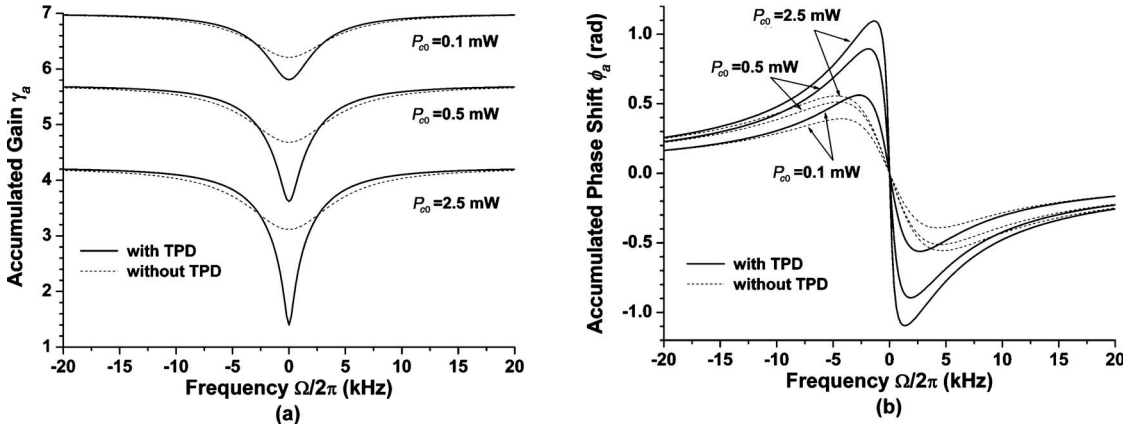

Fig. 2. (a) Accumulated gain spectra and (b) accumulated phase shift spectra for the cases with $P_{c0}=0.1$, 0.5, and 2.5 mW.

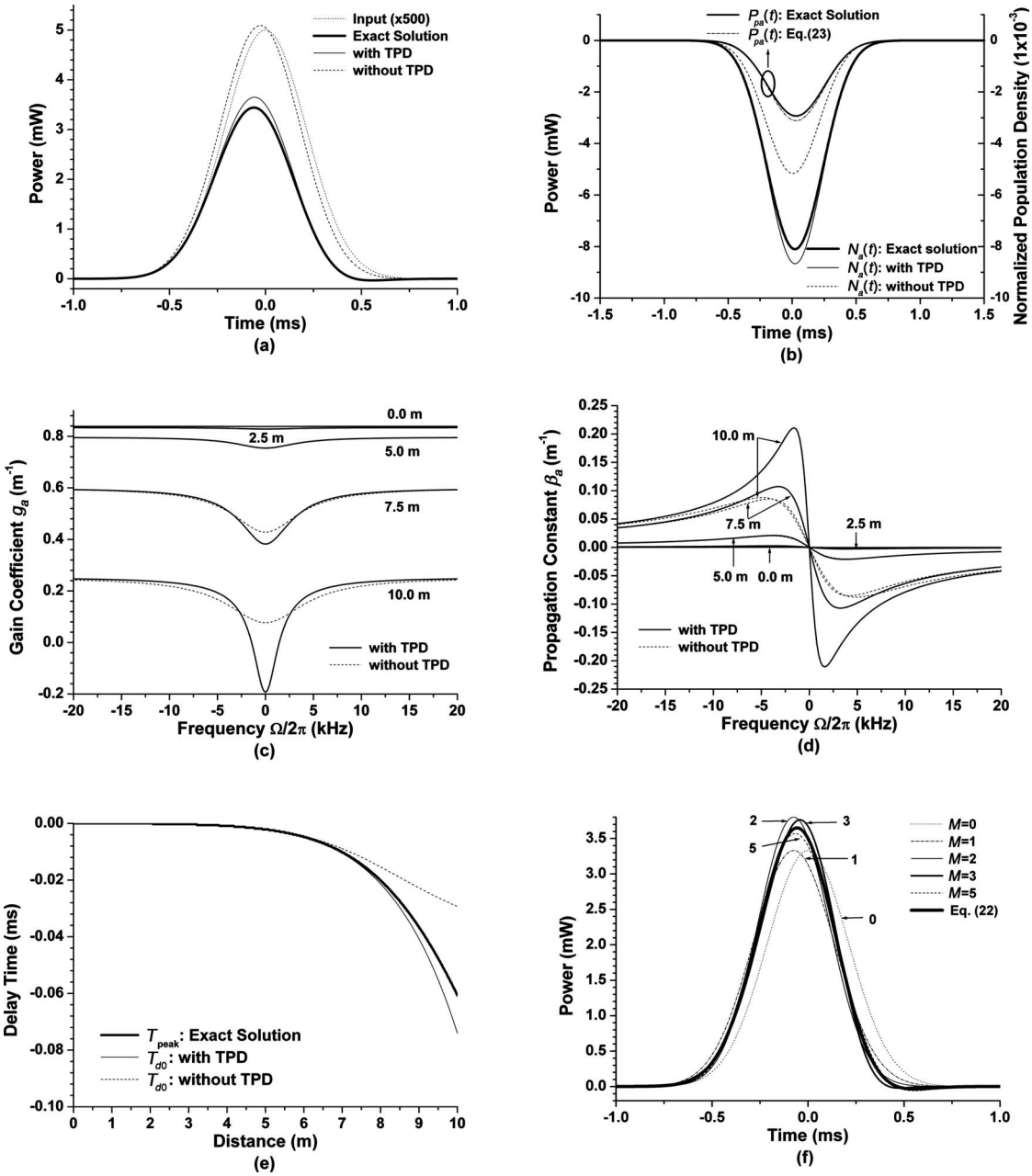

Fig. 3. Same as Fig. 1 except that input control beam power $P_{c0}=0.1$ mW.

crease the pulse delay time and slow down fast light. Therefore, the group velocity of fast light cannot be defined as the velocity derived from the slope of propagation constant at $\Omega=0$. In Figs. 1(e) and 1(f), one can see the significant modification of group velocity by high-order dispersions.

It is interesting to note that, comparing $P_a^{(2)}(t)$ with $P_a^{(1)}(t)$ shown in Fig. 1(f), one can see that the second-order gain dispersion significantly narrows the pulse width. It can easily be derived that if there only exists the second-order gain dispersion, the output FWHM pulse width of the Gaussian input pulse given by Eq. (7) is

$$T_{w2}=2[\ln(2)|T_0^2-2\gamma_{a2}|]^{1/2}. \tag{26}$$

If $\gamma_{a2}<T_0^2/2$, the pulse width is narrowed; otherwise, it is broadened. For the case shown in Fig. 1(f), $T_0=0.3$ ms ($T_w=0.5$ ms) and $\gamma_{a2}=0.0569$ ms^2. We have $T_{w2}=0.256$ ms, and the pulse is significantly compressed. The compressed pulse width enhances the unsymmetric pulse shape distortion due to the third-order dispersion in which $\phi_{a3}=0.0257$ ms^3. The dispersions of order higher than the third-order smooth out the oscillating tail of $P_a^{(3)}(t)$. The resulting FWHM pulse width is 0.42 ms. In general the pulse width may be broadened or narrowed depending on system parameters, such as pulse width, control beam power, and pump power [13]. Under a small signal assumption, dispersion coefficients change with the control beam and pump powers.

B. $P_{c0}=0.1$ mW

With a lower P_{c0}, the depletion of pump power by the amplified control beam power is less, and the recovery of the

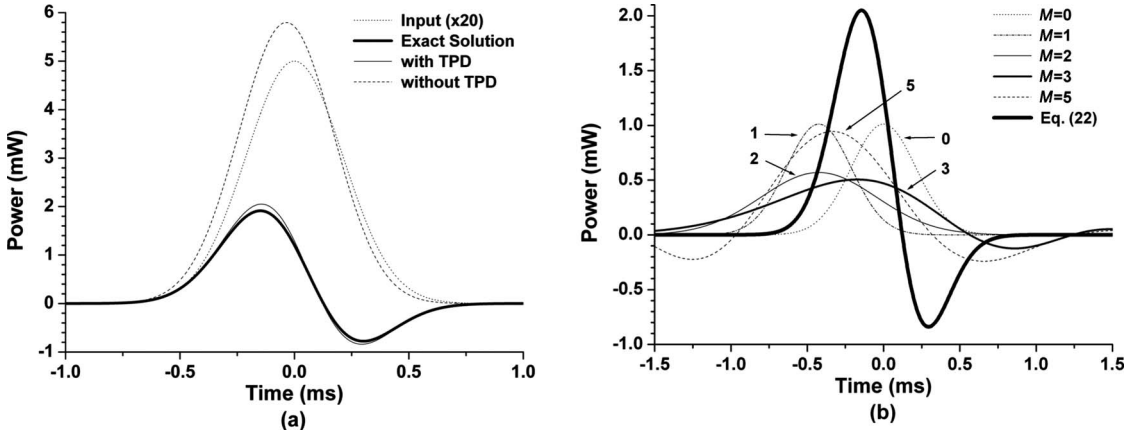

Fig. 4. With input control beam power $P_{c0}=2.5$ mW, (a) input and output pulse shapes and (b) output pulse shapes $P_a^{(M)}(t)$ synthesized up to several M dispersion orders and the approximate solution with TPD calculated from Eq. (22) without dispersion expansion. (b) Corresponding values of M (arrows). The exact solution is solved from Eqs. (1)–(3). (a) Approximate solutions with and without TPD are shown for comparison.

metastable population density (gain) is better. This results in less pulse shape distortion but a slowing down of fast light induced by CPO. Figures 3(a)–3(f) show the same numerical results as Figs. 1(a)–1(f), respectively, except that $P_{c0}=0.1$ mW and the input pulse shape is enlarged 500 times in Fig. 3(a). Comparing Fig. 3(a) with Fig. 1(a), one can see that the output pulse shape is better maintained, and the absolute value of the pulse delay time is decreased as expected. Comparing Fig. 3(b) with Fig. 1(b), one can see that the depletion of the pump power and metastable population density by the pulse are larger because of a higher pulse gain and output pulse power. In Fig. 3(c), at 2.5 and 5 m distances, the gain coefficients for the cases with and without TPD are about the same because the pulse power is still low and TPD is not yet significantly built up, as are the propagation constant spectra shown in Fig. 3(d). At a 7.5 m distance, TPD is high enough so that the difference between the cases with and without TPD becomes apparent. In Fig. 3(e), we have average group indexes $n_{\text{avg}}=-1794$, -2223, and -877 for the peak-power delay time T_{peak}, T_{d0} with TPD, and T_{d0} without TPD, respectively.

Figures 2(a) and 2(b) also show the accumulated gain and phase shift, respectively, for the case with $P_{c0}=0.1$ mW. The wide bandwidth of the gain dip for this case decreases the high-order dispersions so that the pulse shape is better maintained. For this case, $\gamma_{a2}=0.0105\ \text{ms}^2$, we have $T_{w2}=0.438$ ms from Eq. (26), and the pulse compression owing to γ_{a2} is slight. In Fig. 3(f), one can see that, including only up to the fifth-order dispersion, $P_a^{(5)}(t)$ is about the same as the pulse shape calculated from Eq. (22). The resulting FWHM pulse width is slightly narrowed and is 0.472 ms. Fast light slowed down due to the third-order dispersion is less significant than the case with $P_{c0}=0.5$ mW.

C. $P_{c0}=2.5$ mW

From the results shown above, it seems that we may enhance the average negative group index and increase the absolute value of the pulse delay time by increasing P_{c0}. However the increase of the input control beam power not only enhances the first-order dispersion coefficient ϕ_{a1} but also higher-order dispersion coefficients ϕ_{ak} $(k>1)$. The enhanced higher-order dispersion coefficients may result in a serious pulse shape distortion and slowing down of fast light. For example, Figs. 4(a) and 4(b) show the same case as Figs. 1(a) and 1(f), respectively, except that $P_{c0}=2.5$ mW, and the input pulse shape is enlarged 20 times in Fig. 4(a). One can see that $\phi_{a1}=-0.424$ ms, which is about an 85% pulse width, but the combined effect of higher-order dispersions decreases the peak-power delay time to be -0.144 ms (-4320 average group index) and seriously distorts the pulse shape. In Fig. 4(b), one can see that $P_a^{(2)}(t)$ is broadened instead of narrowed. For this case, $\gamma_{a2}=0.187\ \text{ms}^2$, which is large enough to broaden the pulse width. From Eq. (26), $T_{w2}=0.888$ ms. Careful system parameter optimization is able to improve the absolute value of the peak-power delay time under a certain constraint of the pulse shape distortion [13]. However, as the first-order dispersion is enhanced, higher-order dispersions are usually enhanced accordingly. The optimization should compromise between the first-order dispersion and higher-order dispersions.

5. CONCLUSIONS

Fast light can be realized by utilizing the CPO effect in an EDFA in which a pulse superimposed on a strong cw control beam is launched into the EDFA. The pulse depletes the metastable population density. The pump power is absorbed more when the metastable population density is depleted. In literature, the perturbation method analyzing fast light in an EDFA did not consider this pump power depletion. Thus the CPO effect is underestimated, and the derived gain coefficient and propagation constant are inaccurate. We have developed the perturbation method for solving the time varying parts of the signal power, pump power, and metastable population density. The coupled equations of the spectral components of the

signal power, pump power, and metastable population density are derived. From the coupled equations, we can accurately solve the gain coefficient and propagation constant of fast light in an EDFA. It is found that the pulse gain and the absolute value of the negative group velocity are over estimated if TPD is not considered. From the solved gain coefficient and propagation constant, we also study the pulse delay time and shape distortion resulting from high-order dispersions induced by CPO. The gain dispersion resulting from accumulated gain is shown. Accumulated gain is the integration of the gain coefficient along an EDFA, which is an even function of frequency. The second-order gain dispersion may symmetrically broaden or compress the pulse depending on the value of its coefficient. The changes of the pulse shape by higher even order gain dispersions are complicated because of the combined effect with high-/odd-order phase shift dispersions. The phase shift dispersion results from the accumulated phase shift, which is the integration of the propagation constant along an EDFA and is an odd function of frequency. The first-order phase shift dispersion undistortedly leads to a negative pulse delay time. Higher-/odd-order phase shift dispersions unsymmetrically distort the pulse shape and change the pulse delay time. For the shown examples, the third- and fifth-order dispersions result in slowing down and accelerating fast light, respectively. Thus the group velocity of fast light cannot be simply defined as the velocity derived from the first derivative of the propagation constant. The presented perturbation method can also be applied to analyze fast light in other resonant mediums with optical pumping.

ACKNOWLEDGMENT

This work was supported in part by Chung Hua University, China, under contract CHU-95-TR-01.

REFERENCES

1. R. Y. Chiao, "Superluminal (but casual) propagation of wave packets in transparent media with inverted atomic populations," Phys. Rev. A **48**, R34–R37 (1993).
2. E. L. Bolda, J. C. Garrison, and R. Y. Chiao, "Optical pulse propagation at negative group velocities due to a nearby gain line," Phys. Rev. A **49**, 2938–2947 (1994).
3. L. V. Hau, S. E. Haris, Z. Dutton, and C. H. Behroozi, "Light speed reduction to 17 meters per second in an ultracold atomic gas," Nature **397**, 594–598 (1999).
4. L. J. Wang, A. Kuzmmich, and A. Dogariu, "Gain-assisted superluminal light propagation," Nature **406**, 277–279 (2000).
5. Md. A. I. Talukder, Y. Amagishi, and M. Tomita, "Superluminal to subluminal transition in the pulse propagation in a resonant absorbing medium," Phys. Rev. Lett. **86**, 3546–3549 (2001).
6. M. S. Bigelow, N. N. Lepeshkin, and R. W. Boyd, "Observation of ultraslow light propagation in a ruby crystal at room temperature," Phys. Rev. Lett. **90**, 113903 (2003).
7. M. S. Bigelow, N. N. Lepeshkin, and R. W. Boyd, "Ultraslow and superluminal light propagation in solids at room temperature," J. Phys. Condens. Matter **16**, R1321–R1340 (2004).
8. G. Dolling, C. Enkrich, M. Wegener, C. M. Soukoulis, and S. Linden, "Simultaneous negative phase and group velocity of light in a metamaterial," Science **312**, 892–894 (2006).
9. A. Schweinsberg, N. N. Lepeshkin, M. S. Bigelow, R. W. Boyd, and S. Jarabo, "Observation of superluminal and slow light propagation in erbium-doped optical fiber," Europhys. Lett. **73**, 218–224 (2006).
10. G. M. Gehring, A. Schweinsberg, C. Barsi, N. Kostinski, and R. W. Boyd, "Observation of backward pulse propagation through a medium with a negative group velocity," Science **312**, 895–897 (2006).
11. E. Desurvire, *Erbium-Doped Fiber Amplifiers, Principles and Applications* (Wiley, 1994).
12. R. Boyd, *Nonlinear Optics*, 2nd ed. (Elsevier, 2003).
13. H. Shin, A. Schweinsberg, G. Gehring, K. Schwertz, H. J. Chang, R. W. Boyd, Q.-H. Park, and D. J. Gautheir, "Reducing pulse distortion in fast-light pulse propagation through an erbium-doped fiber amplifier," Opt. Lett. **32**, 906–908 (2007).